Optimization of multistage turbines using a through-flow code

M V Petrovic[1], **G S Dulikravich**[2*] and **T J Martin**[3]
[1]Faculty of Mechanical Engineering, The University of Belgrade, Yugoslavia
[2]Department of Mechanical and Aerospace Engineering, The University of Texas at Arlington, Texas, USA
[3]Department of Aerospace Engineering, The Pennsylvania State University, University Park, Pennsylvania, USA

Abstract: Fast and accurate flow calculation and performance prediction of multistage axial flow turbines at design and off-design conditions were performed using a compressible steady state inviscid through-flow code with high fidelity loss and mixing models. The code is based on a stream function model and a finite element solution procedure. A new design system has been developed which optimizes hub and shroud geometry and inlet and exit flow field parameters for each blade row of a multistage axial flow turbine. Optimization was performed using a hybrid constrained optimization code that switches among the modules automatically in order to avoid local minima and to accelerate design convergence rate. By automatically varying a relatively small number of geometric variables per turbine stage it is possible to find an optimal radial distribution of flow parameters at the inlet and outlet of every blade row. Thus, an optimized meridional flow path can be found that is defined by the optimized shape of the hub and shroud while keeping blade shapes intact. The multistage design optimization system has been demonstrated using an actual two-stage axial gas turbine as an example. The comparison of computed performance of an already very high efficiency initial design and its optimized design demonstrates more than 1 per cent improvement in the turbine efficiency at design and significant off-design conditions. The entire design optimization process is feasible on a typical single-processor computer workstation or a personal computer.

Keywords: axial turbines, through flow, optimization, aerodynamic design, aerodynamics

NOTATION

c	absolute velocity
h	static enthalpy
h^0	total enthalpy
$\bar{h}$	relative blade height, fraction of span
$\dot{m}$	mass flowrate
Ma	Mach number
n	rotational speed (r/min)
n_S	number of stages
p	pressure
R	radius
Re	Reynolds number
s	entropy
t	blade pitch
T	temperature
u	tangential velocity
z	axial coordinate
α	absolute flow angle (from tangential direction)
β	relative flow angle (from tangential direction)
δ	thickness, clearance height
ζ	loss coefficient
η	efficiency
θ	deflection angle
π	pressure ratio
ψ	stream function
ω	angular velocity (s^{-1})

Subscripts

Cl	clearance
in	inlet
m	mean radius
out	outlet

This paper was presented at the ASME Turbo-Expo-2000 held in Munich, Germany on 8–11 May 2000 as ASME paper 2000-GT-0521. The MS was received on 11 January 2001 and was accepted after revision for publication on 29 May 2001.
**Corresponding author: Department of Mechanical and Aerospace Engineering, The University of Texas at Arlington, Box 19018, Arlington, TX 76019, USA.*

r	radial component
s	isentropic
tt	total to total
TE	trailing edge
u	tangential component
z	axial component
1	stator outlet
2	rotor outlet

1 INTRODUCTION

Multidisciplinary inverse design [**1**, **2**] and optimization design [**3**] methods that are currently developed for turbomachinery applications incorporate aerodynamic, thermal and structural calculation procedures [**4**, **5**]. Most of the early work focused on optimization of one-dimensional pitchline design (for example, reference [**6**]). This technique gives the optimum geometry of the row at mean diameter and is widely used for preliminary turbomachinery design. There were also early attempts at optimizing multistage axial compressor meridional planes [**7**] and a highly analytical approach at optimizing inlet and exit boundary conditions for each blade row in an axial turbine [**8**]. Massardo *et al.* [**9**] used a through-flow code to optimize the spanwise distribution of an axial compressor blade geometry. Egorov *et al.* [**10**, **11**] used a sophisticated stochastic optimization algorithm to suggest means for improving a multistage axial compressor performance. Cravero and Dawes [**12**] presented a concept for optimizing the design conditions of an axial turbine stage. The objective was to find a radial distribution of absolute swirl velocity at the inlet and exit of a stator blade row and a rotor blade row that will minimize the overall single-stage aerodynamic losses. They used a standard streamline curvature through-flow analysis code having standard loss correlations. A simple polynomial parametrization of the swirl velocity and the stator and rotor blade lean angles were used. For optimization, they used a rudimentary gradient search constrained minimization routine.

Petrovic *et al.* [**13**, **14**] expanded on this general idea by demonstrating a highly accurate and fast method of maximizing efficiency of multistage axial gas turbines by utilizing a high fidelity through-flow analysis code and a robust hybrid constrained optimizer. The method automatically determines an optimal shape variation of hub and shroud without changing the original blade shapes. As a by-product, it also automatically determines an optimal radial distribution of flow angles at the inlet and exit of every blade row. The optimized solution provides for maximum multistage axial turbine efficiency. The design system was demonstrated on experimentally tested single-stage and two-stage axial gas turbines.

Once the optimized inlet and exit boundary conditions of each blade row are found, a relatively inexpensive method of detailed inverse shape design of the entire three-dimensional blade [**15**] or shape optimization of two-dimensional airfoil cascades in each blade row [**16**] can be performed subject to the optimized inlet and exit boundary conditions. On the basis of these new detailed blade shapes, it should be possible to repeat the optimization of hub and shroud shapes and inlet and exit boundary conditions, thus optimizing the shape of the loss coefficient radial profile and further improving the turbine efficiency.

2 THROUGH-FLOW ANALYSIS CODE

A through-flow analysis method will be used as a cost-effective alternative to a full three-dimensional multistage Navier–Stokes flow analysis code. The through-flow code was developed by Petrovic [**17**]. It is based on a classical through-flow theory [**18**] but includes significant improvements and extensions. It is basically an inviscid code with a high fidelity distributed loss model. A finite element procedure with eight-node isoparametric quadrilateral elements and biquadratic interpolation functions was applied to solve the distribution of a stream function in a turbine meridional surface. The loss model developed by Traupel [**19**] was adapted to two-dimensional calculations and applied in order to compute the loss coefficient and the entropy increase. New models for realistic radial distribution of losses, spanwise mixing, two-dimensional deviation and off-design flow loss prediction have been developed and introduced in order to achieve high accuracy of the code. An important feature has been added to encompass far off-design flow phenomena (flow separation and flow reversal) and low load operation at which the turbine's last stage or a part of it works with power consumption. All applied models are based on a large amount of experimental data thus enabling them to predict main flow losses very accurately. More details about the analytical background of the method and applied loss and mixing model are given in a paper by Petrovic and Riess [**20**].

This through-flow code is able to calculate axisymmetric flow fields in axial multistage gas turbines and steam turbines at subsonic and transonic conditions. It can accurately and very quickly predict the flow field and the turbine performance at the design load and over a wide range of partial loads. The reliability of the method was verified by comparing the calculations with the experimental results for several gas and steam turbines [**20–22**]. The comparisons of numerical results with results of extensive experimental investigation show very close agreement.

The through-flow code can be used in two modes: analysis and design. In the analysis mode, the flow field (distribution of p, T, h, s and velocity vector components) on a meridional surface and turbine overall performance are calculated for the specified turbine geometry and fixed values of blade row inlet and outlet angles. For optimization purposes, the through-flow code has been rewritten in a design mode, in which the radial distribution of the tangential velocity component is fixed. The flow angle and turbine efficiency can then be calculated.

3 CONSTRAINED HYBRID OPTIMIZATION ALGORITHM

The design space for a typical optimization problem of this type has a number of local minima. A typical gradient-based optimization algorithm would quickly terminate in the nearest local minimum which might not even satisfy all of the specified constraints. In order to avoid the local minima, it is advantageous to use a constrained evolutionary hybrid optimization approach [**2–5**, **23**]. The hybrid constrained algorithm used in this work incorporated four of the most popular optimization approaches: a genetic algorithm, the Nelder–Mead simplex method, simulated annealing and the Davidon–Fletcher–Powell gradient search method. Each time when a local minimum was detected, automatic switching logic was used to change to another optimization algorithm. Details of this algorithm are explained in a publication by Dulikravich *et al.* [**3**]. The hybrid optimizer treated the existence of constraints in three ways: Rosen's projection method, a feasible search and random design generation. Rosen's projection method provided search directions which guided the descent direction tangent towards active constraint boundaries. In the feasible search, designs that violated constraints were automatically restored to feasibility via the minimization of the active global constraint functions. If at any time this constraint minimization failed, a number of random designs were generated using a Gaussian-shaped probability density cloud about a desirable and feasible design until a new design was reached. This hybrid constrained optimizer accepts an arbitrary number of equality and inequality constraints.

4 DESIGN OPTIMIZATION

The goal of the present optimization is to find the optimal shape of the hub and the shroud and radial distribution of inlet and outlet flow angles of every blade row that will provide for the maximum turbine efficiency η_{tt} where

$$\eta_{tt} = \frac{\Delta h + c_{in}^2/2 - c_{out}^2/2}{\Delta h_s + c_{in}^2/2 - c_{out}^2/2}$$

Since the optimization algorithm is defined to minimize a scalar function, the objective function in this case is $f_{obj} = -\eta_{tt}$. During the hub and shroud geometry optimization process, turbine mass flowrate $\dot{m}$, total enthalpy drop Δh^0 and rotational speed n are kept constant. An updated version of Traupel's loss model [**17**] was implemented in the through-flow code to compute the flow losses. In this model, the correlations for profile, secondary and clearance losses are functions of geometrical and flow parameters.

An analysis of loss correlations suggests that turbine stage efficiency is a function of geometric parameters (mean radius R_m, blade height h, pitch t, clearance radius R_{Cl} and height δ_{Cl}, trailing edge thickness δ_{TE}, chord length) and flow parameters (inlet and outlet flow angles β_1, β_2, deflection θ, Mach and Reynolds numbers Ma, Re, incidence angle and velocity vectors). Some of these parameters (δ_{Cl}, δ_{TE}) have to be fixed. The others are not independent: velocities, Ma and Re are functions of flow angles, mean radius and blade height. Also, inlet angle is a function of the outlet angle of the previous row and of the incidence angle. Consequently, four parameters need to be optimized for each stage of the multistage turbine: radial distribution of flow angles and axial distribution of mean radius and blade height.

However, it is easier to optimize the variation of the following four parameters per stage of the multistage machine:

(a) $c_{u1}(R)$ = tangential component of velocity at stator outlet;
(b) $c_{u2}(R)$ = tangential component of velocity at rotor outlet;
(c) $R_{Hub}(z)$ = hub radius;
(d) $R_{Shroud}(z)$ = shroud radius.

From the optimized values of $c_{u1}(R)$ and $c_{u2}(R)$ it is easy to determine the corresponding optimized spanwise distribution of angles.

The axial variation of hub and shroud radii can be described by two spline functions [**24**], $R_{Hub}(z)$ and $R_{Shroud}(z)$. For simplicity, only four geometrical parameters per stage for hub and four geometrical parameters per stage for shroud were used. This can be easily changed to an arbitrary spline representation of the hub and shroud.

Tangential components of velocities at stator and rotor exits were described, similarly to Cravero and Dawes [**12**], by fourth-degree polynomials as a function of relative blade height ($0.0 < \bar{h} < 1.0$). This representation needs the following ten parameters:

$$c_{u1} = A_1 + B_1\bar{h} + C_1\bar{h}^2 + D_1\bar{h}^3 + E_1\bar{h}^4 \quad (1)$$

$$c_{u2} = A_2 + B_2\bar{h} + C_2\bar{h}^2 + D_2\bar{h}^3 + E_2\bar{h}^4 \quad (2)$$

One of these ten parameters can be obtained from a condition that the turbine total enthalpy drop remains constant during the design optimization process. This means that for a single-stage machine the integral of the Euler equation over mass flowrate has to be constant for every combination of flow and geometric parameters:

$$\Delta h^0 = \int_0^1 (u_1 c_{u1} - u_2 c_{u2})\, \mathrm{d}\psi = \text{constant} \tag{3}$$

Replacing c_{u1} and c_{u2} in equation (3) with the polynomials (1) and (2) gives

$$\Delta h^0 = A_1 \omega (I_1 - I_2) \tag{4}$$

$$I_1 = \int_0^1 R\left(1 + \frac{B_1}{A_1}\,\bar{h} + \frac{C_1}{A_1}\,\bar{h}^2 + \frac{D_1}{A_1}\,\bar{h}^3 + \frac{E_1}{A_1}\,\bar{h}^4\right) \mathrm{d}\psi \tag{5}$$

$$I_2 = \int_0^1 R\left(\frac{A_2}{A_1} + \frac{B_2}{A_1}\,\bar{h} + \frac{C_2}{A_1}\,\bar{h}^2 + \frac{D_2}{A_1}\,\bar{h}^3 + \frac{E_2}{A_1}\,\bar{h}^4\right) \mathrm{d}\psi \tag{6}$$

$$A_1 = \frac{\Delta h^0}{\omega (I_1 - I_2)} \tag{7}$$

The stream function, ψ, and radius, R, are functions of the relative blade height, $\bar{h}$. This means that there are finally nine flow parameters to optimize the tangential components of velocities at stator and rotor outlets of a single stage:

$$\frac{B_1}{A_1}, \frac{C_1}{A_1}, \frac{D_1}{A_1}, \frac{E_1}{A_1}, \frac{A_2}{A_1}, \frac{B_2}{A_1}, \frac{C_2}{A_1}, \frac{D_2}{A_1}, \frac{E_2}{A_1} \tag{8}$$

In summary, the total number of parameters to optimize for every turbine stage is 17 (eight geometrical and nine flow parameters).

In the case of a multistage turbine, the distribution of the turbine enthalpy drop over the stages can also be optimized while satisfying the following condition

$$\Delta h^0 = \sum_{i=1}^{n_S} \Delta h_{Si}^0 = \text{constant} \tag{9}$$

where n_S is the number of turbine stages, Δh_{Si}^0 is the enthalpy drop of stage i and Δh^0 is the turbine total enthalpy drop. In that case, there are an additional $n_S - 1$ parameters to optimize. If the enthalpy drop of every stage is known, the same procedure [equations (3) to (8)] should be performed for every stage in order to find the corresponding set of nine flow parameters.

The first optimization cycle (iteration) starts with a detailed initial turbine geometry and input flow data: $\dot{m}$, T_{in}, p_{in}. The through-flow code in its analysis mode then evaluates the overall performance of the initial configuration and initiates Δh_{Si}^0 and the distribution of c_{u1} and c_{u2} for every stage. The optimizer then delivers an improved set of geometrical (axial distribution of hub and shroud radii) and flow (radial distribution of c_{u1} and c_{u2}) parameters. A new finite element grid is then automatically generated for the meridional flow field surface. The through-flow code in its design mode then runs with the new distributions of c_{u1} and c_{u2}, thus creating a new set of flow parameters. The result is the spanwise distribution of flow angles at the inlet and outlet of every blade row and the overall turbine efficiency. Depending on the achieved η_{tt}, the optimizer enters the next iterative cycle by generating an improved set of parameters and the iterative optimization process is repeated until the maximum of efficiency is achieved (Fig. 1).

By running the through-flow code in its analysis mode, the overall efficiency of the optimized configuration over a wide range of part loads is then calculated in order to check the optimized turbine performance at off-design conditions. If the overall efficiency of the optimized configuration at all expected operating conditions is acceptable, the design optimization process is finished.

The iterative design process runs fully automatically. The designer's task is to prepare the input data and to set constraints for design variables. The flow variables are usually allowed to vary without any limits. The variation of the rotor blade tip radius is often limited by the

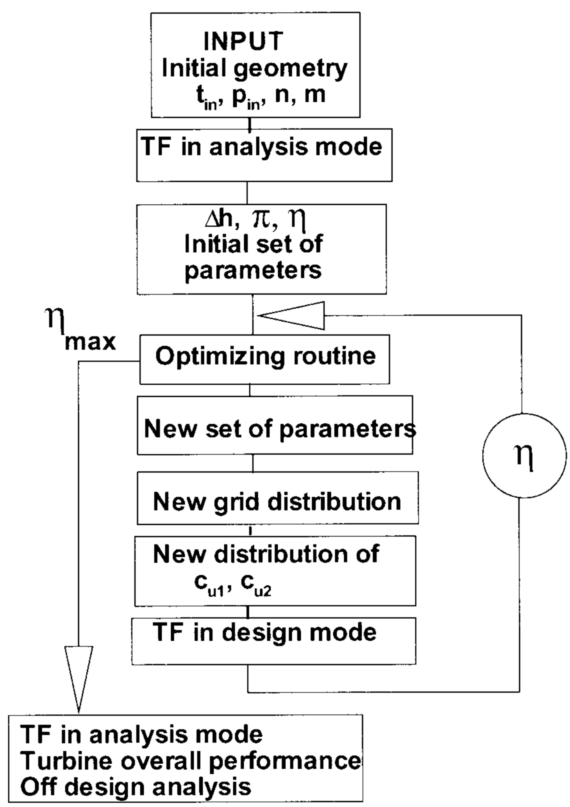

Fig. 1 Optimization algorithm

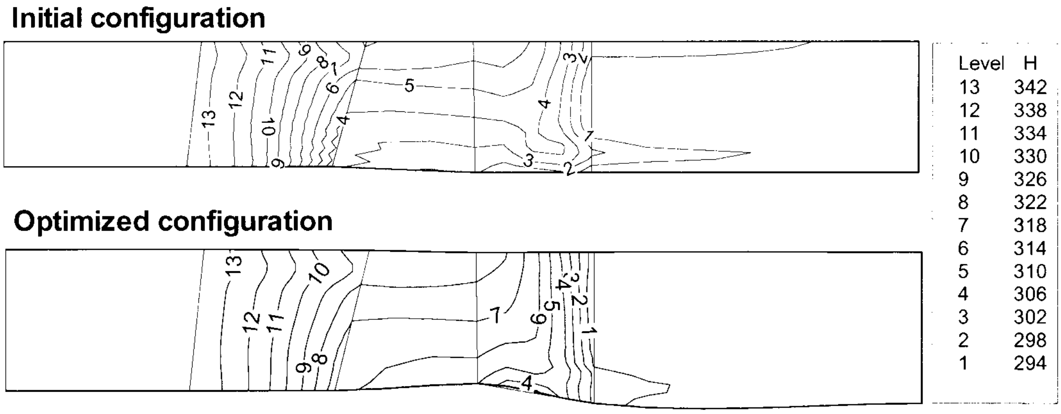

Fig. 2 Enthalpy fields of initial and optimized single-stage turbine

maximum stress at the rotor root, i.e. by the maximum allowed tangential velocity if the rotating speed is fixed.

5 EXAMPLES OF TURBINE OPTIMIZATION

The first reported use of this turbine design methodology was an example [**13**] involving a single-stage uncooled transonic axial gas turbine that was experimentally tested by Foerster and Kruse [**25**]. At the design conditions, the calculated value of turbine efficiency was $\eta_{tt} = 0.8952$, while the experimentally measured value was $\eta_{tt} = 0.8940$ thus confirming the high accuracy of the through-flow code. The multistage design optimization method was able to increase the maximum efficiency of this turbine to $\eta_{tt,opt} = 0.9154$. Although optimized for a single design operating point, the part load behaviour of the optimized turbine was significantly better over a wide range of load. Only at very far off-design conditions did the initial configuration show higher efficiency.

Later, on improving the optimizer search algorithm and the connection between the optimizer and the through-flow code, the turbine performance has been improved further. The efficiency of the new optimized configuration was $\eta_{tt,opt} = 0.9175$. This represents an absolute improvement of approximately $\Delta\eta_{tt} = 2.2$ per cent. Also, at part load the new turbine was better over the entire operating range than the initial configuration.

Figures 2 to 4 depict the initial and the optimized shapes of the hub and the shroud and the corresponding field distributions of enthalpy, Mach number and entropy at the turbine design operating conditions.

The next example is a two-stage uncooled NASA axial turbine that was experimentally tested and described by Whitney *et al.* [**26**]. This well-documented set of experimental data has been used to check the accuracy of numerical results and to demonstrate the capability of the proposed multistage turbine design optimization system. The turbine was intended for high temperature engine application. The turbine had a mean diameter of 660.4 mm. The mean blade height in the first stage was 100 mm. The blade height in the second stage was 134.6 mm at the stator outlet and 148.6 mm at the rotor outlet. Equivalent design speed was $N/\sqrt{\theta_{cr}} = 4407.36$ r/min where θ_{cr} is the squared ratio of critical speed at turbine inlet to critical speed of sea level air. The turbine operated at an overall pressure ratio ranging from

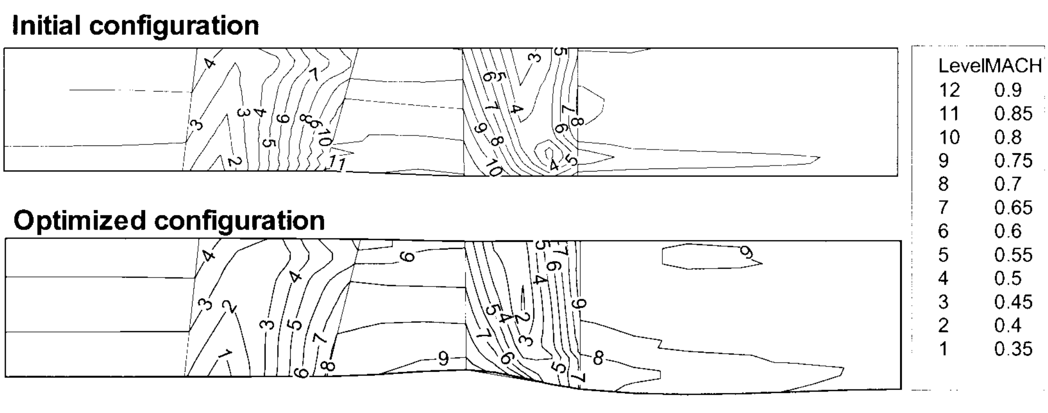

Fig. 3 Mach number fields of initial and optimized single-stage turbine

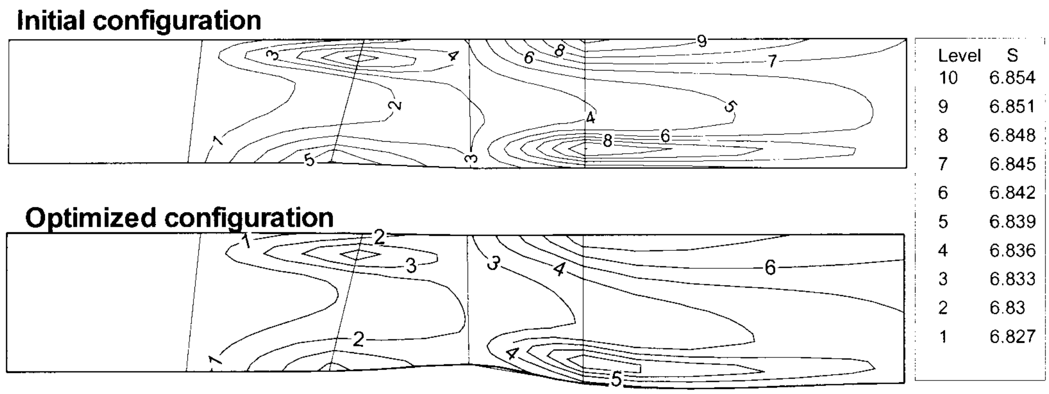

Fig. 4 Entropy fields of initial and optimized single-stage turbine

1.4 to 4.0. The design pressure ratio was $\pi_0 = 3.2$. The experimentally measured efficiency of the initial configuration was already extremely high: $\eta_{tt} = 0.9320$. To check the through-flow code accuracy in its analysis mode, a calculation of the turbine flow at the nominal rotating speed was performed. At the design conditions, the through-flow analysis code predicted the value of turbine efficiency as $\eta_{tt} = 0.9307$ (Fig. 5), while the experimentally measured value was $\eta_{tt} = 0.9320$ [**25**].

Next, the two-stage turbine was optimized while keeping constant rotational speed, mass flowrate, total enthalpy drop, number and shapes of blades, rotor tip clearance, blade chord lengths and blade trailing edge thicknesses. Only a small increase of the first rotor tip diameter and no increase of the second rotor tip diameter were allowed. A polynomial spline discretization of the hub and shroud geometry was performed using the radii indicated in Fig. 6 as design variables.

The through-flow code in its design mode needed approximately 15 s to find each flow field solution on a personal computer with 400 MHz processor. The grid refinements study was performed to make computing time shorter. It was concluded that the use of ten elements in the radial direction and three elements per blade row in the axial direction gives very good results. Thus, the applied computational grid had only 250 elements. Here, the finite element method with eight-node isoparametric quadrilateral elements and biquadratic interpolation functions was used. In this particular example where the initial two-stage axial turbine already had an

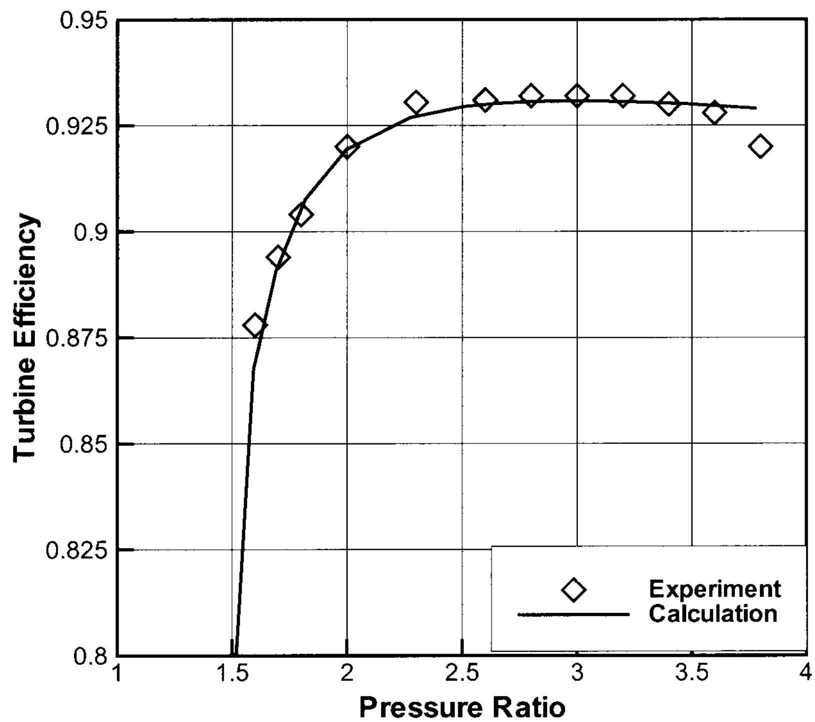

Fig. 5 Efficiency of two-stage turbine at design rotating speed

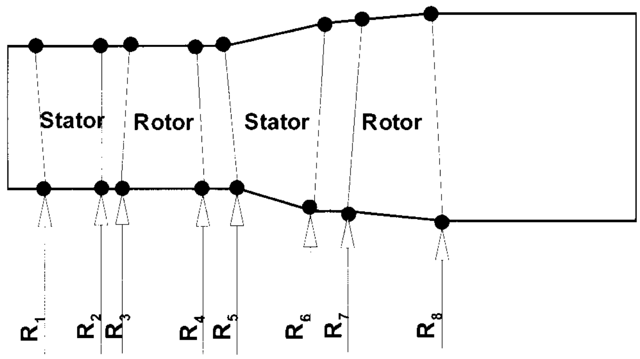

Fig. 6 Hub and shroud discretization of the two-stage turbine

extremely high efficiency, about 2000 through-flow runs in the design mode were necessary to find the turbine stage configuration that gives the maximum total-to-total efficiency. This would have consumed an unacceptable amount of computing time if a fully three-dimensional multistage Navier–Stokes flow field analysis code was used instead of the fast augmented through-flow code. It was assumed that both blade count and radial variation of chord lengths have already been determined by some preliminary design procedure (e.g. meanline optimization). Conceptually, it would be possible to include both of these parameters and other design parameters deemed to be influential in the multistage efficiency optimization.

The resulting optimized meridional flow path became significantly different in comparison with the initial flow path (Fig. 7). The corresponding maximum computed value for the optimized turbine efficiency was increased to $\eta_{tt,opt} = 0.9424$. This represents an improvement of $\Delta\eta_{tt} = 1.17$ per cent over the efficiency of the initial configuration ($\eta_{tt,init} = 0.9307$). Figure 8 demonstrates the superior performance of the optimized configuration over the entire range of operating conditions when compared with the performance of the initial turbine configuration.

The changes in tangential components of velocity are presented in Fig. 9. Comparisons of spanwise distributions of blade exit metal angles, flow losses, reaction and stage efficiency for the initial and the optimized configuration are presented in Figs 10 and 11. Figure 12 shows the computed flow field entropy distribution in the initial and the optimized configuration.

It can be seen that it was not possible to reduce the flow loss coefficient in the turbine blade rows (Fig. 11). Even in the hub region of the first stator and in the shroud region of the first rotor, the loss coefficients are higher owing to increase of the clearance radii. A reduction of secondary loss coefficient was possible in the second rotor in both hub and shroud regions (Fig. 11). The flow losses and the entropy increase have been reduced (Fig. 12) by a more suitable distribution of the enthalpy drop between stator and rotor in both stages. This was achieved by decreasing the tangential absolute velocity component at the exit of the blade rows (Fig. 9), i.e. by changing the metal outlet angles of the blades (Fig. 11). The degree of reaction has been increased in the second stage and slightly decreased in the first stage (Fig. 10). The optimized configuration has a degree of reaction at the blade mean radius of approximately 0.35 in the first stage and 0.60 in the second stage. The efficiency of both stages was definitely improved (Fig. 10).

6 CONCLUSIONS

A design system for multistage axial turbine hub and shroud geometry optimization has been developed. The system uses a fast and accurate through-flow aerodynamics analysis code and a robust constrained optimization algorithm. The analysis of loss models has indicated that there are at least 17 parameters per turbine stage that could be optimized: eight geometrical parameters to describe the shapes of the hub and the shroud and nine flow field parameters to describe the spanwise variation of tangential component of velocity at stator and rotor exits. By varying these 17 parameters per turbine stage, the optimization code automatically searches for the flow field and the turbine hub and shroud geometry that give the maximum efficiency. This design system has been successfully applied to optimization of the meridional

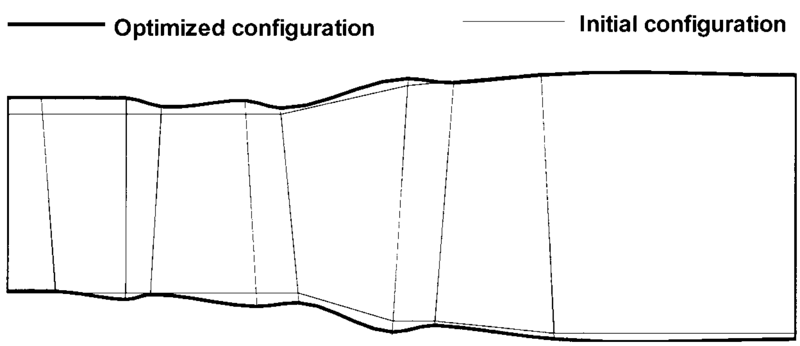

Fig. 7 Initial and optimized meridional flow paths in the two-stage turbine

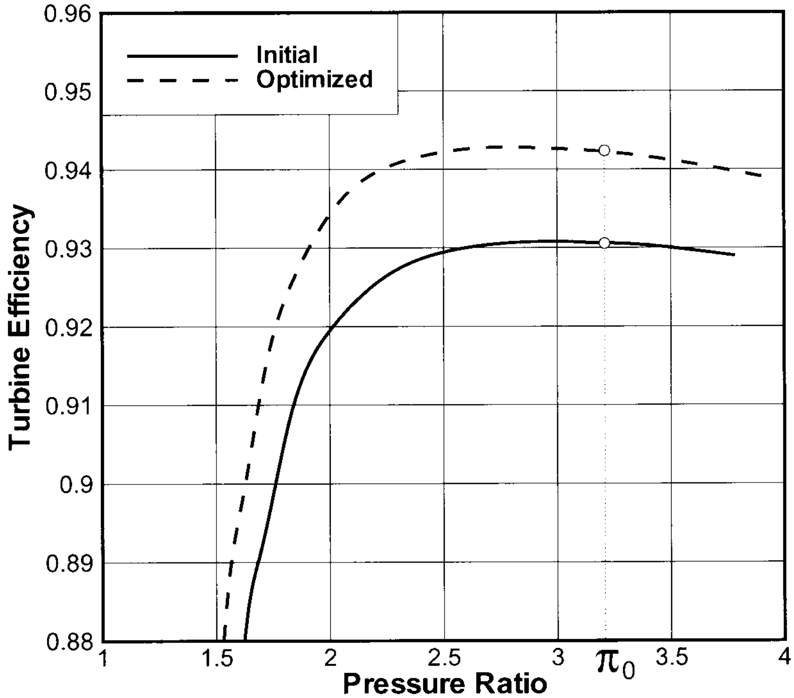

Fig. 8 Calculated initial and optimized efficiency variations of the two-stage turbine ($\pi_0 = 3.2$ is the design pressure ratio)

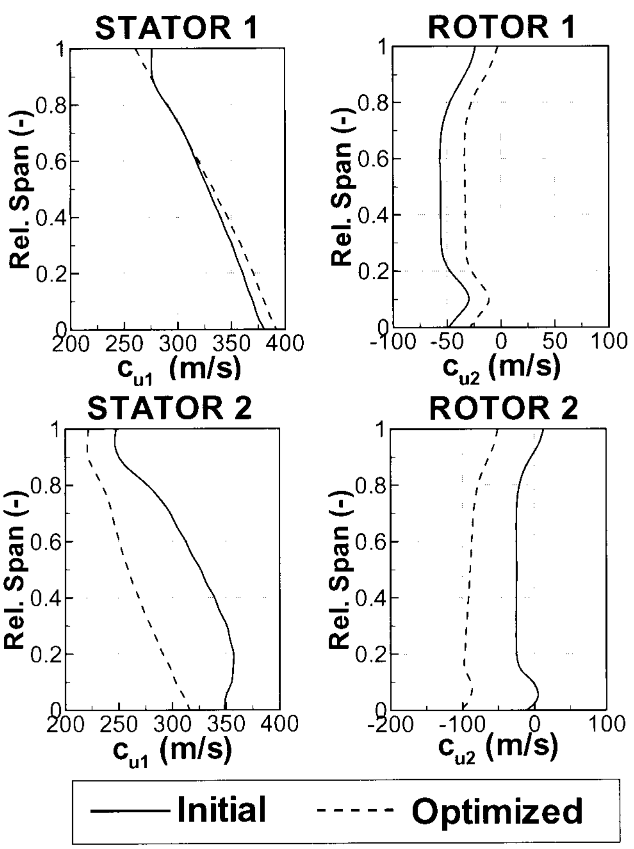

Fig. 9 Spanwise distribution of blade exit tangential velocities in the initial and the optimized two-stage turbine configurations

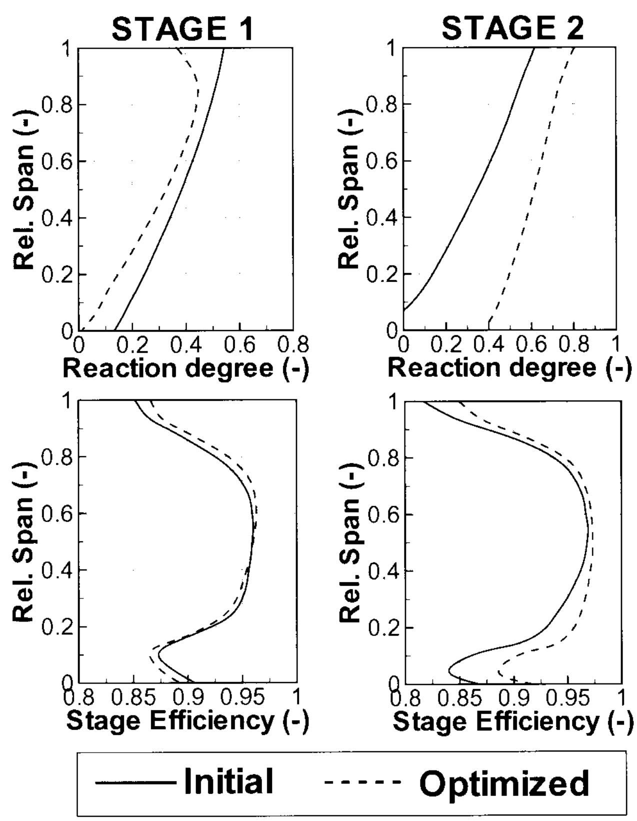

Fig. 10 Comparison of reaction and stage efficiency along the blade span in the initial and the optimized two-stage turbine configurations

flow path and radial distribution of circumferential mean flow angles in a two-stage axial gas turbine. The achieved efficiency of the optimized configuration was 1.17 per cent better than the efficiency of the initial configuration at the design load. The through-flow code in an analysis mode was applied to analyse off-design behavior of the optimized configuration which was found to perform better over the entire range of loads compared with the initial configuration. The same design optimization procedure is applicable to multistage steam turbines.

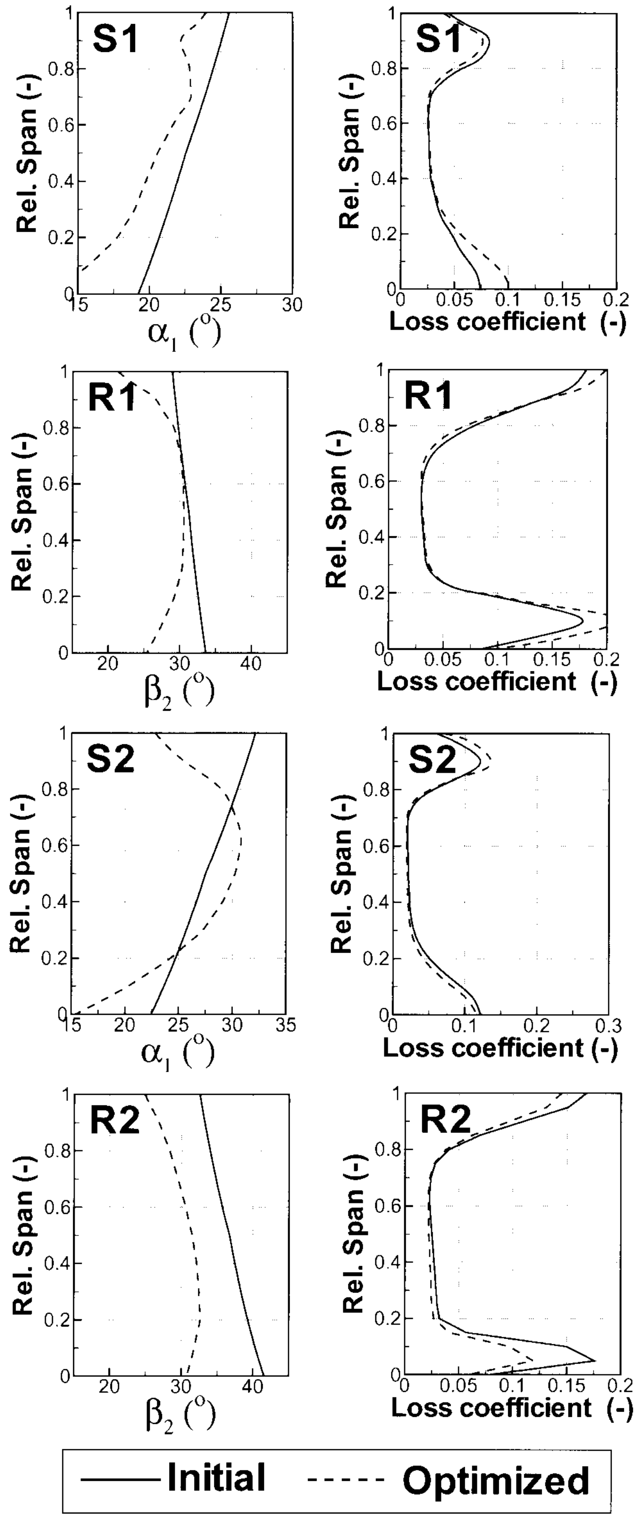

Fig. 11 Spanwise distribution of blade exit metal angles and flow losses, in the initial and the optimized configurations

ACKNOWLEDGEMENTS

The authors are grateful for National Science Foundation Grants DMI-9522854 and DMI-9700040 monitored by Dr George Hazelrigg, for NASA Glenn Research Center Grant NAG3-1995 facilitated by Dr John Lytle and Dr Herbert J. Gladden and monitored by Dr Kestutis Civinskas and for a Lockheed Martin Skunk Works grant monitored by Mr Thomas Oatway.

REFERENCES

1 **Fujii, K.** and **Dulikravich, G. S.** (Eds) *Recent Development of Aerodynamic Design Methodologies—Inverse Design and Optimization*, Vieweg Series on Notes on Numerical Fluid Mechanics, Vol. 68, April 1999 (Springer-Verlag, Berlin).

2 **Dulikravich, G. S., Martin, T. J.** and **Dennis, B. H.** Multidisciplinary inverse problems. Invited lecture in Third International Conference on *Inverse Problems in Engineering (3icipe)* (Ed. K. Woodbury), Port Ludlow, Puget Sound, Washington, 13–18 June 1999.

3 **Dulikravich, G. S., Martin, T. J., Dennis, B. H.** and **Foster, N. F.** Multidisciplinary hybrid constrained GA optimization. Invited lecture in *Evolutionary Algorithms in Engineering and Computer Science: Recent Advances and Industrial Applications (EUROGEN '99)* (Eds K. Miettinen, M. M. Makela, P. Neittaanmaki and J. Periaux), Jyvaskyla, Finland, 30 May–3 June 1999, Ch. 12, pp. 231–260 (John Wiley, New York).

4 **Martin, T. J.** and **Dulikravich, G. S.** Aero-thermal analysis and optimization of internally cooled turbine blades. In XIII International Symposium on *Airbreathing Engines (XIII ISABE)*, Chattanooga, Tennessee, 1997, ISABE 97-7165, Vol. 2, pp. 1232–1250.

5 **Dulikravich, G. S., Martin, T. J., Dennis, B. H., Lee, E.-S.** and **Han, Z.-X.** Aero-thermo-structural design optimization of cooled turbine blades. In AGARD–AVT Propulsion and Power Systems Symposium on *Design Principles and Methods for Aircraft Gas Turbine Engines*, Toulouse, France, 11–15 May 1998, NATO-RTO-MP-8 AC/323(AVT)TP/9, Ch. 35.

6 **Balje, O.** and **Binsley, H.** Axial turbine performance evaluation. *Trans. ASME, J. Engng Pwr*, 1968, **90**, 341–360.

7 **Biagosch, A.** Verfahren zur Optimierung der aerothermodynamischen Auslegung mehrstufiger Axialverdichter. Dissertation, University of Munich, Germany, 1984.

8 **Lurie, K. A., Fedorov, A. V.** and **Klimovich, V. I.**

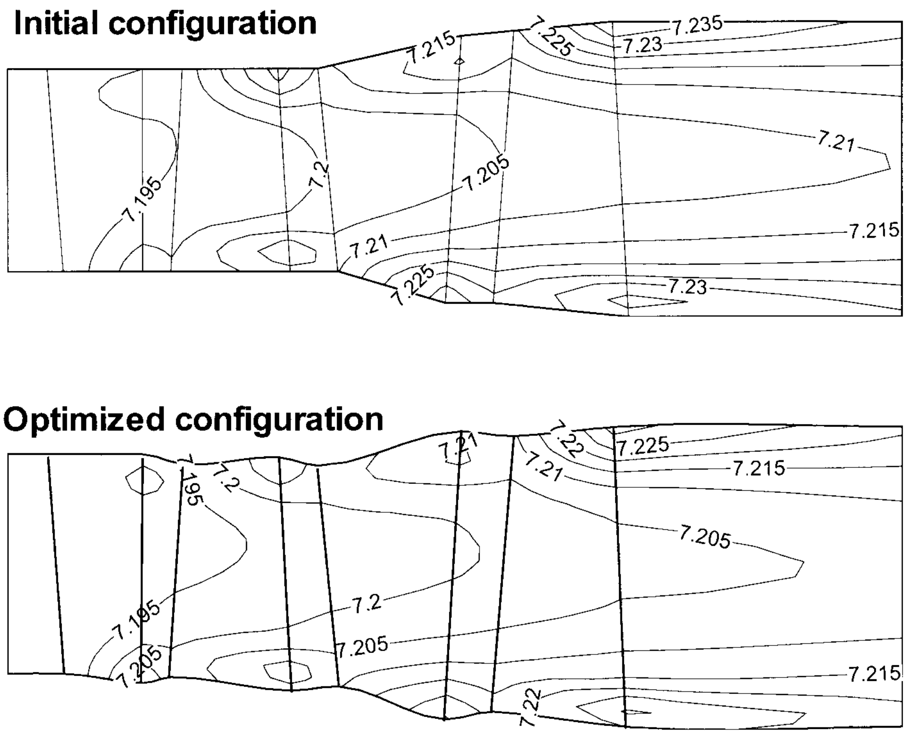

Fig. 12 Calculated entropy distribution in initial and optimized two-stage axial gas turbine configurations

Conditions along the boundaries of bladed zones within the flow tracts of turbines. *Int. J. Numer. Meth. Fluids*, 1982, **2**, 299–311.

9 **Massardo, A., Satta, A.** and **Marini, M.** Axial flow compressor design optimisation: Part II—throughflow analysis. *Trans. ASME, J. Turbomachinery*, 1990, **112**, 406–410.

10 **Egorov, I. N., Fomin, V. N.** and **Talyzina, V. S.** Numerical method of optimization of a multistage axial compressor. In First ISAIF Proceedings, Beijing, PR China, 1990.

11 **Egorov, I. N., Kretinin, G. V., Talyzina, V. S.** and **Leshchenko, I. A.** Multistage axial flow compressor's development on the basis of the numerical optimization methods. In *Aerothermodynamics of Internal Flows III*, 1996, pp. 104–112 (World Publishing, Beijing, PR China).

12 **Cravero, C.** and **Dawes, W. N.** Throughflow design using an automatic optimisation strategy. In ASME Turbo Expo, Orlando, Florida, 2–5 June 1997, paper 97-GT-294.

13 **Petrovic, M. V., Dulikravich, G. S.** and **Martin, T. J.** Maximizing multistage turbine efficiency by optimizing hub and shroud shapes and inlet and exit conditions of each blade row. In ASME Turbo Expo, Indianapolis, Indiana, 7–10 June 1999, ASME paper 99-GT-071; also *Int. J. Turbo Jet Engines*, 2000, **17**, 267–278.

14 **Petrovic, M., Dulikravich, G. S.** and **Martin, T. J.** Maximizing multistage gas turbine efficiency over a range of operating conditions. In Proceedings of 10th Thermal and Fluids Analysis Workshop (*TFAWS'99*) (Ed. L. W. Griffin), NASA Marshall Space Flight Center, Huntsville, Alabama, 13–17 September 1999.

15 **Dulikravich, G. S.** and **Baker, D. P.** Aerodynamic shape inverse design using a Fourier series method. In AIAA Aerospace Sciences Meeting, Reno, Nevada, 11–14 January 1999, AIAA paper 99-0185.

16 **Dennis, B. H., Dulikravich, G. S.** and **Han, Z.-X.** Constrained optimization of turbomachinery airfoil cascade shapes using a Navier–Stokes solver and a genetic/SQP algorithm. In ASME Turbo Expo, Indianapolis, Indiana, 7–10 June 1999, ASME paper 99-GT-441; also *Am. Inst. Aeronaut. Astronaut. J. Propulsion Pwr*, 2001, **17**(5), 1123–1128.

17 **Petrovic, M.** Berechnung der Meridianstroemung in mehrstufigen Axialturbinen bei Nenn- und Teillastbetrieb. In *Stroemungstechnik*, Fortschritt-Berichte VDI, Reiche 7, No. 280, 1995 (VDI, Dusseldorf).

18 **Hirsch, C.** and **Deconinck, H.** Through flow models for turbomachines: stream surface and passage averaged representations. In *Thermodynamics and Fluid Mechanics of Turbomachinery*, Vol. I (Eds A. S. Ucer, P. Stow and C. Hirsch), 1985 (Nijhoff, Dordrecht).

19 **Traupel, W.** *Thermische Turbomaschinen*, Vol. I, 1988 (Springer-Verlag, Berlin).

20 **Petrovic, M.** and **Riess, W.** Off-design flow analysis and performance prediction of axial turbines. In ASME Turbo Expo, Orlando, Florida, June 2–5, June 1997, ASME paper 97-GT-55.

21 **Petrovic, M.** and **Riess, W.** Off-design flow analysis of LP steam turbines. *Proc. Instn Mech. Engng, Part A, Journal of Power and Energy*, 1997, **211**(A3), 215–223.

22 **Petrovic, M.** and **Riess, W.** Through-flow calculation in axial flow turbines at part load and low load. In 1st European Conference on *Turbomachinery—Fluid Dynamic and Thermodynamic Aspects*, Erlangen, Germany, 1995.

23 **Foster, N. F.** and **Dulikravich, G. S.** Three-dimensional

aerodynamic shape optimization using genetic and gradient search algorithms. *Am. Inst. Aeronaut. Astronaut. J. Spacecraft and Rockets*, 1997, **34**(1), 36–42.

24 **Akima, H.** A new method of interpolation and smooth curve fitting based on local procedures. *J. Ass. Comput. Machinery*, 1970, **17**, 589–602.

25 **Foerster, W.** and **Kruse, H.** Test case E/TU-3, single stage subsonic turbine. In *AGARD AR 275: Test Cases for Computation of Internal Flows in Aero Engine Components* (Ed. L. Fottner), 1990.

26 **Whitney, W. J., Schum, H. J.** and **Behning, F. P.** Cold-air invesigation of a turbine for high-temperature-engine application. NASA TN D-6960, 1972.